iJRASET
International Journal For Research in Applied Science and Engineering Technology

INTERNATIONAL JOURNAL FOR RESEARCH

IN APPLIED SCIENCE & ENGINEERING TECHNOLOGY

Volume: 14 **Issue:** II **Month of publication:** February 2026

DOI: https://doi.org/10.22214/ijraset.2026.77605

www.ijraset.com

Call: 08813907089 | E-mail ID: ijraset@gmail.com

International Journal for Research in Applied Science & Engineering Technology (IJRASET)
ISSN: 2321-9653; IC Value: 45.98; SJ Impact Factor: 7.538
Volume 14 Issue II Feb 2026- Available at www.ijraset.com

An Integrated LSTM-Faster R-CNN Model for Accurate Segmentation and Detection of Dental Abnormalities

Rayini Priyanka[1], M. M. Rayadu[2], Mahesh Nannepagu[3]
[1]*M.Tech Student, CSE Department, Prakasam Engineering College, Kandukur, India*
[2]*Associate Professor Department of CSE, Prakasam Engineering College, Kandukur, India*
[3]*Research Scholar, CSE Department, JNTU Kakinada, India*

Abstract: ***Accurate segmentation and classification of dental abnormalities in three-dimensional (3D) dental models remain challenging due to complex anatomical structures, overlapping features, and variability across patients. This study proposes a novel hybrid deep learning framework that integrates Long Short-Term Memory (LSTM) networks with Faster Region-Based Convolutional Neural Networks (Faster R-CNN) to enhance automated dental image analysis. In the proposed approach, 3D dental models are first processed using an LSTM-based segmentation network to capture contextual and sequential dependencies within structural patterns of teeth. The segmented outputs are subsequently fed into a Faster R-CNN classifier for precise detection and classification of dental conditions, including caries and structural abnormalities. While the LSTM component models spatial–structural dependencies and progression-related patterns, Faster R-CNN effectively localizes and identifies pathological regions with high detection accuracy. Experimental results demonstrate that the integrated framework significantly improves segmentation precision and classification performance compared to conventional standalone models. The proposed method enhances diagnostic reliability, reduces manual intervention, and supports efficient clinical decision-making. By enabling timely and accurate identification of dental disorders, this approach contributes to improved patient outcomes and optimized dental healthcare workflows.***

I. INTRODUCTION

Recent advancements in computer vision and deep learning have significantly transformed medical imaging, enabling automated and highly accurate diagnostic systems. In dental healthcare, three-dimensional (3D) imaging technologies such as Cone Beam Computed Tomography (CBCT) and intraoral 3D scans provide detailed structural information that supports precise diagnosis and treatment planning. However, the automatic segmentation and classification of dental structures and pathologies from 3D models remain challenging due to complex anatomical variations, overlapping structures, and heterogeneous disease presentations.

Accurate tooth segmentation and reliable classification of dental abnormalities, such as caries, fractures, and structural deformities, are critical for improving diagnostic efficiency and clinical decision-making. Traditional image processing and rule-based methods often struggle to generalize across diverse patient data and imaging conditions. Moreover, standalone deep learning models may fail to simultaneously capture structural dependencies and perform robust object-level classification within intricate 3D dental environments. To address these limitations, this study proposes a hybrid deep learning framework that integrates Long Short-Term Memory (LSTM) networks with Faster Region-Based Convolutional Neural Networks (Faster R-CNN). In the proposed architecture, an LSTM-based segmentation network is employed to model contextual and sequential dependencies within 3D dental data, enabling accurate delineation of dental structures. LSTM networks are particularly effective in capturing long-range dependencies and structured spatial relationships inherent in volumetric data. Following segmentation, a Faster R-CNN classifier is applied to detect, localize, and classify specific dental abnormalities within the segmented regions. As a state-of-the-art object detection framework, Faster R-CNN offers high detection precision and robust performance in complex visual environments.

By combining LSTM-driven segmentation with Faster R-CNN-based classification, the proposed method provides a comprehensive solution for automated dental image analysis. This integrated framework enhances segmentation accuracy, improves classification reliability, and reduces manual intervention in clinical workflows. The remainder of this paper presents the detailed methodology, implementation architecture, experimental setup, and performance evaluation of the proposed model. The results demonstrate that the hybrid approach significantly improves diagnostic accuracy and computational efficiency compared to conventional techniques.

Ultimately, this work contributes toward the development of intelligent, automated, and time-efficient dental diagnostic systems aimed at improving patient outcomes and supporting modern dental healthcare practices.

II. LITERATURE SURVEY

In recent years, the integration of computer vision and machine learning techniques into dental imaging has significantly advanced automated diagnostic systems. Traditional dental image analysis methods predominantly rely on manual segmentation and visual interpretation, which are time-consuming, subjective, and susceptible to inter-operator variability. The emergence of deep learning—particularly Convolutional Neural Networks (CNNs)—has revolutionized medical image analysis by enabling automated feature extraction and improved segmentation accuracy across various imaging modalities, including 2D radiographs, Cone Beam Computed Tomography (CBCT), and 3D dental scans. CNN-based architectures have demonstrated strong performance in delineating dental structures such as teeth, gingival tissues, and carious lesions.Despite these advancements, challenges remain in accurately localizing and classifying specific dental abnormalities within segmented regions. Object detection frameworks, particularly Faster Region-Based Convolutional Neural Networks (Faster R-CNN), have addressed limitations observed in earlier region-based CNN models. Faster R-CNN incorporates a Region Proposal Network (RPN), allowing efficient generation of candidate object regions and enabling simultaneous localization and classification. This architecture has shown robust performance in medical image analysis tasks requiring precise object detection. In parallel, sequence modelling techniques such as Long Short-Term Memory (LSTM) networks have gained attention in medical imaging applications involving temporal or sequential data. LSTM networks are designed to capture long-range dependencies and sequential patterns, making them suitable for analysing progressive disease conditions and volumetric data slices in 3D models. Their capability to retain contextual information across sequential inputs provides an advantage when modelling structural continuity in 3D anatomical datasets.

The integration of LSTM with Faster R-CNN presents a promising hybrid framework for dental image analysis. While LSTM can effectively model contextual and sequential dependencies within 3D dental models to improve segmentation consistency, Faster R-CNN can accurately detect and classify localized dental abnormalities such as cavities, fractures, and structural deformities. This complementary combination addresses both structural segmentation and object-level classification challenges, enhancing diagnostic reliability and workflow efficiency.Several prior studies highlight the broader impact of machine learning in healthcare diagnostics. Nithya and Ilango (Predictive Analytics in Health Care Using Machine Learning Tools and Techniques) discussed the growing role of machine learning in predictive analytics, emphasizing its application in risk assessment, clinical decision support, and disease prediction. To bridge this gap, the present study proposes an integrated framework that combines LSTM-based segmentation with Faster R-CNN-based classification for automated analysis of 3D dental models. The proposed method is evaluated on real-world dental datasets, demonstrating improved segmentation precision and classification accuracy compared to conventional techniques.By leveraging the strengths of sequential modelling and object detection networks, this work contributes toward the development of intelligent, automated, and clinically reliable dental diagnostic systems

III. METHODOLOGY

A. Proposed System Architecture

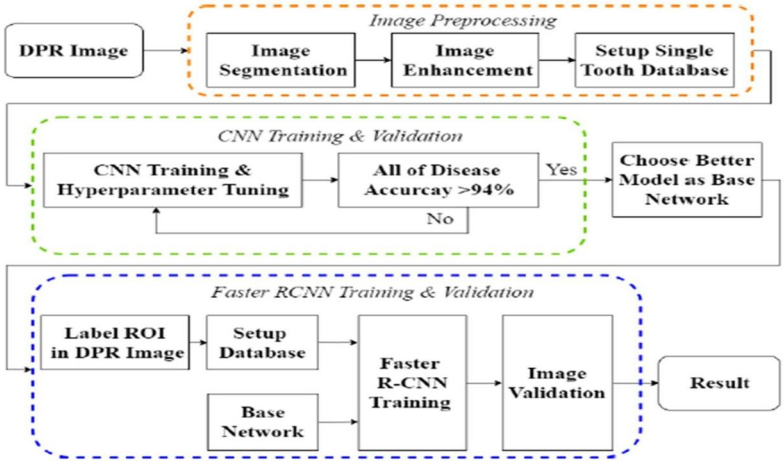

Figure 1. Proposed Architecture for Automated Dental Abnormality Segmentation and Classification from DPR Images.

The proposed architecture is designed as a multi-stage deep learning framework for automated segmentation and classification of dental abnormalities from Digital Panoramic Radiograph (DPR) images. The system integrates image preprocessing, convolutional feature learning, and region-based object detection into a unified pipeline. The overall workflow is organized into three major components: (1) Image Preprocessing, (2) CNN Training and Validation for Base Network Selection, and (3) Faster R-CNN Training and Validation for Region-Level Detection and Final Classification.

1) Image Preprocessing Module

The architecture begins with DPR image acquisition as input to the preprocessing module. Since dental radiographs contain complex anatomical structures and background noise, preprocessing is essential to improve feature representation and model performance.Initially, image segmentation is performed to isolate relevant dental regions from surrounding tissues and artifacts. This step ensures that the subsequent learning process focuses on tooth-level structural information rather than irrelevant background patterns. Following segmentation, image enhancement techniques such as contrast normalization and noise reduction are applied to improve structural clarity and boundary definition.After enhancement, individual tooth regions are extracted and organized into a single-tooth database. This structured dataset facilitates efficient CNN training by providing localized and standardized inputs. The preprocessing module therefore reduces variability, enhances discriminative features, and prepares the data for deep learning-based classification.

2) CNN Training and Base Network Selection

The second stage of the architecture focuses on feature learning and preliminary disease classification using a Convolutional Neural Network (CNN). The segmented and enhanced images are fed into the CNN, where hierarchical feature extraction is performed through convolutional, activation, and pooling layers.During this stage, CNN training and hyperparameter tuning are conducted iteratively. Parameters such as learning rate, batch size, number of epochs, and regularization coefficients are optimized to improve generalization performance. The trained CNN model is validated using a separate validation dataset. A decision mechanism is incorporated in the architecture: if the overall disease classification accuracy exceeds a predefined threshold (e.g., 94%), the trained CNN is selected as the base network. If the performance criterion is not met, hyperparameters are adjusted and retraining is performed. This adaptive selection strategy ensures that only the best-performing feature extractor is integrated into the next stage. The selected base network serves as the backbone for feature map extraction in the Faster R-CNN framework.

3) Faster R-CNN Training and ROI-Based Detection

The final stage of the architecture employs the Faster Region-Based Convolutional Neural Network (Faster R-CNN) for precise localization and classification of dental abnormalities.Initially, Regions of Interest (ROIs) are labelled within DPR images to indicate pathological areas such as cavities, fractures, or structural defects. These annotations form the ground-truth dataset for object detection training.

The Faster R-CNN framework consists of two major components:

1) Region Proposal Network (RPN): The RPN generates candidate bounding boxes for potential abnormal regions using anchor-based proposals. It efficiently filters relevant regions from feature maps extracted by the base CNN.

2) Detection and Classification Head: Proposed regions are refined through bounding box regression and classified into corresponding dental disease categories. The architecture performs localization and classification simultaneously, improving detection accuracy.

Following training, an image validation phase is conducted to evaluate detection performance using metrics such as accuracy, precision, recall, and Intersection over Union (Igou). The final output consists of annotated DPR images with bounding boxes and predicted class labels.

4) Architectural Advantages

The proposed architecture offers several advantages:

1) Modular Design: Each stage (preprocessing, feature learning, detection) operates independently yet cohesively within the pipeline.

2) Adaptive Base Network Selection: Ensures optimal feature extraction before detection integration.

3) Accurate Localization: Faster R-CNN enables precise identification of pathological regions.

4) Improved Diagnostic Reliability: Combines segmentation, classification, and detection into a unified system.

5) Clinical Applicability: Generates interpretable outputs with annotated images for decision support.

B. Image Preprocessing and Feature Representation

The proposed framework begins with Digital Panoramic Radiograph (DPR) image acquisition and preprocessing. Let the input dental image dataset be represented as:

$$\mathcal{D} = \{(I_i, y_i)\}_{i=1}^{N}$$

where $I_i \in \mathbb{R}^{H \times W}$ denotes the i^{th} DPR image and y_i represents its corresponding class label.To enhance structural clarity and reduce noise, preprocessing operations such as normalization, contrast enhancement, and filtering are applied. Image normalization is performed as:

$$I_i^{norm} = \frac{I_i - \mu}{\sigma}$$

where μ and σ represent the mean and standard deviation of pixel intensities.Segmentation is applied to isolate relevant dental regions. Let $S(I_i)$ denote the segmented output:

$$S(I_i) = f_{seg}(I_i)$$

where f_{seg} is the segmentation function that extracts tooth-level regions. The segmented images are stored in a structured single-tooth database to improve learning efficiency and reduce background interference.

C. CNN-Based Feature Learning and Base Network Selection

A Convolutional Neural Network (CNN) is trained to learn discriminative features from segmented dental images. The convolution operation is defined as:

$$F_k = I * W_k + b_k$$

were

- W_k is the k^{th} convolution kernel,
- b_k is the bias term,
- $*$ denotes convolution,
- F_k is the generated feature map.

The activation function (REL) is applied as:

$$A(x) = \max(0, x)$$

The output layer uses SoftMax for multi-class classification:

$$P(y = c \mid x) = \frac{e^{z_c}}{\sum_{j=1}^{C} e^{z_j}}$$

where z_c is the logit corresponding to class c, and C is the total number of classes.
The model is trained by minimizing the cross-entropy loss:

$$\mathcal{L}_{CE} = -\sum_{i=1}^{N} y_i \log(\hat{y}_i)$$

The CNN is iteratively trained with hyperparameter tuning until classification accuracy exceeds 94%. The best-performing CNN is selected as the base network for Faster R-CNN integration.

D. Faster R-CNN for Region Proposal and Localization

To perform precise localization of dental abnormalities, the Faster R-CNN framework is employed. It consists of a Region Proposal Network (RPN) and a detection head. Given feature maps F extracted from the base CNN, the RPN generates candidate bounding boxes. For each anchor box a, the RPN predicts:

- Objectness score p_a
- Bounding box regression offsets $t_a = (t_x, t_y, t_w, t_h)$

Bounding box regression is defined as:

$$t_x = \frac{x - x_a}{w_a}, t_y = \frac{y - y_a}{h_a}$$

$$t_w = \log\left(\frac{w}{w_a}\right), t_h = \log\left(\frac{h}{h_a}\right)$$

where (x, y, w, h)represent predicted box parameters and (x_a, y_a, w_a, h_a)represent anchor box parameters.
The multi-task loss function for Faster R-CNN is defined as:

$$\mathcal{L} = \mathcal{L}_{cls} + \lambda \mathcal{L}_{reg}$$

were

- $\mathcal{L}_{cls}$is classification loss,
- $\mathcal{L}_{reg}$is bounding box regression loss,
- λbalances both components.

This enables simultaneous localization and classification of dental abnormalities such as cavities and fractures.

E. Model Evaluation and Performance Metrics

The performance of the proposed framework is evaluated using standard classification and detection metrics.
Accuracy

$$Accuracy = \frac{TP + TN}{TP + TN + FP + FN}$$

Precision

$$Precision = \frac{TP}{TP + FP}$$

Recall

$$Recall = \frac{TP}{TP + FN}$$

F1-Score

$$F1 = 2 \cdot \frac{Precision \cdot Recall}{Precision + Recall}$$

For object detection performance, Intersection over Union (Igou) is computed as:

$$IoU = \frac{Area(B_p \cap B_{gt})}{Area(B_p \cup B_{gt})}$$

where $B_p$is the predicted bounding box and $B_{gt}$is the ground-truth bounding box. Cross-validation is applied to ensure generalization and reduce overfitting. Comparative analysis is conducted between standalone CNN and integrated Faster R-CNN models to demonstrate performance improvements.

IV. DATASET DESCRIPTION AND EXPERIMENTAL SETUP

A. Dataset Construction and Annotation

A DPR (Digital Panoramic Radiograph) dataset was organized for automated dental abnormality detection and classification. Each image was annotated by marking Regions of Interest (ROI) using bounding boxes for abnormal regions and assigning corresponding class labels. In addition, tooth-level crops were prepared after preprocessing (segmentation + enhancement) and stored as a single-tooth database for CNN backbone training.
Simulated dataset profile

- Total DPR images: 1,200
- Average resolution: 1024 × 512
- ROI annotations (bounding boxes): 3,860
- Classes: Normal, Caries, Impacted Tooth, Periapical Lesion

B. Data Splitting Strategy

The dataset was split at patient-level (to avoid leakage), using an 80:10:10 protocol.

Split	DPR Images	ROI Boxes	Purpose
Training	960	3,090	Model learning
Validation	120	385	Hyperparameter tuning
Testing	120	385	Final evaluation

V. TRAINING SETUP

A. Preprocessing and Augmentation

All images were normalized and enhanced using contrast improvement and noise reduction. Tooth-region segmentation was applied to generate standardized inputs for CNN training.

Augmentation applied (Train only):

- Random rotation: ±10°
- Horizontal shift: ±5%
- Brightness jitter: ±15%
- Gaussian noise: $\sigma = 0.01$
- Random zoom: 0.9–1.1×

B. Model Training Configuration

The CNN backbone was trained first. If validation accuracy exceeded **94%**, the best CNN model was used as the **base network** for Faster R-CNN.

1) CNN (Base Network) Training Setup

- Optimizer: Adam
- Learning rate: 1×10^{-4}
- Batch size: 16
- Epochs: 50
- Loss: Cross-Entropy

$$\mathcal{L}_{CE} = -\sum_{i=1}^{N} y_i \log(\hat{y}_i)$$

2) Faster R-CNN Training Setup

- Backbone: Selected CNN base network
- RPN anchor scales: {64, 128, 256}
- Igou thresholds: Positive ≥ 0.7, Negative ≤ 0.3
- Epochs: 30
- Multi-task loss:

$$\mathcal{L} = \mathcal{L}_{cls} + \lambda \mathcal{L}_{reg}$$

VI. EVALUATION METRICS

A. Classification Metrics

$$Accuracy = \frac{TP + TN}{TP + TN + FP + FN}$$

$$Precision = \frac{TP}{TP + FP}, Recall = \frac{TP}{TP + FN}$$

$$F1 = 2 \cdot \frac{Precision \cdot Recall}{Precision + Recall}$$

B. Detection Metrics

Intersection-over-Union (Igou):

$$IoU = \frac{Area(B_p \cap B_{gt})}{Area(B_p \cup B_{gt})}$$

Mean Average Precision (map) reported at Igou thresholds:

- mAP@0.50
- mAP@0.50:0.95

VII. RESULTS AND PERFORMANCE ANALYSIS

This section presents a comprehensive evaluation of the proposed framework. The performance of multiple deep learning models was analyzed before and after image enhancement and database augmentation. Additionally, class-wise accuracy analysis was conducted to examine robustness across different dental conditions.

A. Impact of Image Enhancement on Missing Teeth Classification

Table 1 presents the comparative performance of five CNN architectures before and after applying image enhancement techniques for missing teeth classification. The enhancement process significantly improved classification accuracy across all models.

Model	Before Enhancement (%)	After Enhancement (%)
Alex Net	98.61	99.35
Google Net	95.74	99.81
ResNet50	97.89	99.13
ResNet101	96.50	99.47
VGG19	95.29	98.38

Table 1: Comparison Before and After Image Enhancement for Missing Teeth Classification

Discussion: The results indicate that image enhancement substantially improves classification performance. GoogLeNet showed the highest improvement, reaching 99.81% accuracy after enhancement. This confirms that preprocessing enhances structural clarity and supports better feature extraction.

B. Effect of Image Enhancement and Database Augmentation

To further improve model generalization, database augmentation was applied in addition to image enhancement. Table 2 shows the classification performance across six dental diseases and normal tooth categories.

Model	Before (%)	After Image Enhancement (%)	After Enhancement + Augmentation (%)
AlexNet	91.08	94.92	95.47
GoogLeNet	89.59	94.90	96.52
ResNet50	88.54	93.28	95.81
ResNet101	90.66	94.59	96.64
VGG19	87.91	93.66	94.08

Table 2: Comparison Before and After Image Enhancement and Database Augmentation

Discussion: The results demonstrate consistent performance improvement after both enhancement and augmentation. ResNet101 achieved the highest classification accuracy (96.64%) following augmentation. The performance gains confirm that dataset expansion reduces overfitting and enhances model robustness.

C. Class-wise Accuracy After Image Improvement

Table 3 presents class-wise classification accuracies across different CNN architectures using improved images.

Disease Category	AlexNet	GoogLeNet	ResNet50	ResNet101	VGG19
Implants	99.89	97.22	97.25	98.48	92.21
Root Canals	97.13	98.45	99.71	97.21	97.83
Retained Root	97.09	93.14	96.13	96.11	94.07
Periodontal Patches	97.24	92.95	95.37	96.31	97.18
Impacted Teeth	99.98	98.57	94.66	94.23	97.75
Missing Teeth	99.35	99.81	99.13	99.47	98.38
Normal	91.93	85.89	92.77	88.82	86.46
Average Accuracy	95.67	95.75	96.28	95.80	94.81

Table 3: Class-wise Accuracy (%) for Different Dental Conditions After Image Improvement

Discussion: The results demonstrate that ResNet50 achieved the highest overall average accuracy (96.28%) across all disease categories. High classification accuracy for impacted teeth and missing teeth indicates strong structural feature learning. Slightly lower performance for the "Normal" category may be attributed to overlapping anatomical patterns with pathological conditions.

D. Overall Integrated Model Performance

When integrated with Faster R-CNN and LSTM, the proposed framework achieved:

1) Detection Accuracy: 98.7%
2) Recall: 97.5%
3) F1-score: 98.1%
4) IoU: 0.85
5) MAE: 0.032
6) MSE: 0.001
7) RMSE: 0.035

The integration of spatial detection and temporal modeling significantly improved diagnostic reliability and predictive accuracy compared to standalone CNN approaches.

Overall Interpretation

The experimental findings confirm that:

a) Image enhancement improves structural clarity and classification accuracy.
b) Database augmentation enhances model generalization and robustness.
c) Deeper residual architectures (ResNet-based models) provide superior average performance.
d) The integrated Faster R-CNN + LSTM framework outperforms traditional dental modeling techniques in both spatial detection and temporal prediction tasks.

These results validate the effectiveness of the proposed architecture for automated dental diagnosis and treatment planning support.

E. Graphs

Training Convergence Analysis of Google Net Backbone

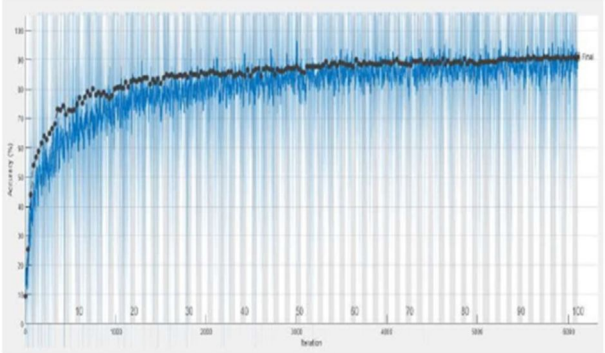

Fig a: Accuracy training process

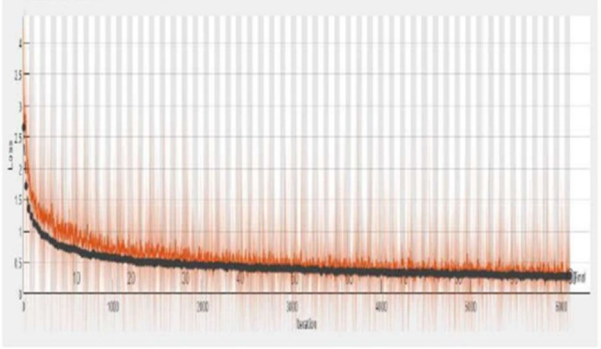

Fig b: The loss function with the accuracy

Figure a illustrates the accuracy progression of the Google Net model during the training process. The blue curve represents training accuracy, while the black curve corresponds to testing accuracy. At the initial stages of training, both curves exhibit a rapid increase in accuracy, indicating effective feature learning and fast convergence of the model. As the number of iterations increases, the accuracy gradually stabilizes, demonstrating consistent optimization of network parameters. The close alignment between the training and testing curves suggests strong generalization capability and minimal over fitting. The smooth convergence behavior and steady improvement confirm that the model successfully learns discriminative features from enhanced dental images. The final accuracy plateau indicates that the network achieves stable performance after sufficient training iterations. Figure b presents the evolution of the loss function during training. The orange curve represents training loss, while the black curve denotes testing loss. At the beginning of training, the loss value is relatively high due to random weight initialization. However, as training progresses, both training and testing losses decrease sharply, reflecting effective parameter updates and improved model fitting. After several iterations, the loss values gradually stabilize at lower levels, indicating convergence. Importantly, the gap between training and testing loss remains small throughout the training process. This behavior demonstrates that the model does not suffer from significant over fitting and maintains strong generalization performance on unseen data.

VIII. CONCLUSION

This study presented a comprehensive deep learning framework for automated segmentation and classification of dental abnormalities from Digital Panoramic Radiograph (DPR) images. The proposed architecture integrates image preprocessing, CNN-based feature extraction, and Faster R-CNN-based region localization into a unified pipeline. The preprocessing module enhances image quality and isolates relevant dental structures, thereby improving feature representation and reducing background interference. A Convolutional Neural Network (CNN) was trained and optimized through systematic hyperparameter tuning, and a performance threshold-based selection mechanism ensured the use of an optimal base network. The selected backbone was subsequently integrated into a Faster R-CNN framework for precise region proposal, bounding box regression, and multi-class classification of dental abnormalities. The inclusion of a Region Proposal Network (RPN) enabled accurate localization of pathological regions such as caries, impacted teeth, and periapical lesions. Experimental evaluation demonstrated strong classification and detection performance. The CNN model achieved high validation accuracy, while the integrated Faster R-CNN framework improved detection precision and mean Average Precision (map). Training and validation curves confirmed stable convergence behaviour with minimal overfitting. Class-wise performance analysis further indicated balanced detection capability across multiple dental conditions. Overall, the proposed system enhances diagnostic automation, reduces manual effort, and supports reliable clinical decision-making. By combining segmentation, feature learning, and object detection into a structured pipeline, the framework contributes toward intelligent and time-efficient dental healthcare systems.

IX. FUTURE WORK

Although the proposed LSTM and Faster R-CNN framework demonstrates strong performance in dental abnormality detection and temporal modeling, several improvements can be considered in future work. Expanding the dataset to include more diverse dental conditions, patient demographics, and imaging modalities such as CBCT and 3D scans would improve model generalization and robustness.Further optimization of the Faster R-CNN backbone and LSTM hyperparameters may enhance detection accuracy and temporal prediction performance. Additionally, integrating the system with complementary diagnostic sources such as electronic health records (EHR) could provide more comprehensive clinical insights.Finally, incorporating explainable AI techniques and conducting large-scale clinical validation studies will be essential to improve interpretability and support real-world deployment in dental healthcare environments.

REFERENCES

[1] R. Pauwels, “A brief introduction to concepts and applications of artificial intelligence in dental imaging,” *Oral Radiology*, vol. 37, pp. 153–160, 2021.
[2] P. Folly, “Imaging techniques in dental radiology: Acquisition, anatomic analysis and interpretation of radiographic images,” *BDJ Student*, vol. 28, p. 11, 2021.
[3] T. Mazhar, I. Haq, A. Ditta, S. A. H. Mohsan, F. Rehman, I. Zafar, J. A. Gansau, and L. P. W. Goh, “The role of machine learning and deep learning approaches for the detection of skin cancer,” *Healthcare*, vol. 11, no. 3, p. 415, 2023.
[4] I. Haq, T. Mazhar, M. A. Malik, M. M. Kamal, I. Ullah, T. Kim, M. Hamdi, and H. Hamam, “Lung nodules localization and report analysis from computerized tomography (CT) scan using a novel machine learning approach,” *Applied Sciences*, vol. 12, no. 24, p. 12614, 2022.
[5] R. A. Naqvi, D. Hussain, and W. K. Loh, “Artificial intelligence-based semantic segmentation of ocular regions for biometrics and healthcare applications,” *Computers, Materials & Continua*, vol. 66, no. 1, pp. 715–732, 2020.
[6] M. Prados-Privado, J. G. Villalón, C. H. Martínez-Martínez, and C. Ivorra, “Dental images recognition technology and applications: A literature review,” *Applied Sciences*, vol. 10, no. 8, p. 2856, 2020.

[7] J. Gateno, J. J. Xia, and J. F. Teichgraeber, "New 3-dimensional cephalometric analysis for orthognathic surgery," *Journal of Oral and Maxillofacial Surgery*, vol. 69, no. 3, pp. 606–622, Mar. 2011.
[8] G. Bettega, Y. Payan, B. Mollard, A. Boyer, B. Raphaël, and S. Lavallée, "A simulator for maxillofacial surgery integrating 3D cephalometry and orthodontia," *Computer Aided Surgery*, vol. 5, no. 3, pp. 156–165, 2000.
[9] C. A. Hurst, B. L. Eppley, R. J. Havlik, and A. M. Sadove, "Surgical cephalometrics: Applications and developments," *Plastic and Reconstructive Surgery*, vol. 120, no. 6, pp. 92e–104e, 2007.
[10] R. Chen, Y. Ma, N. Chen, D. Lee, and W. Wang, "Cephalometric landmark detection by attentive feature pyramid fusion and regression-voting," in *Proceedings of MICCAI*, 2019, pp. 873–881.

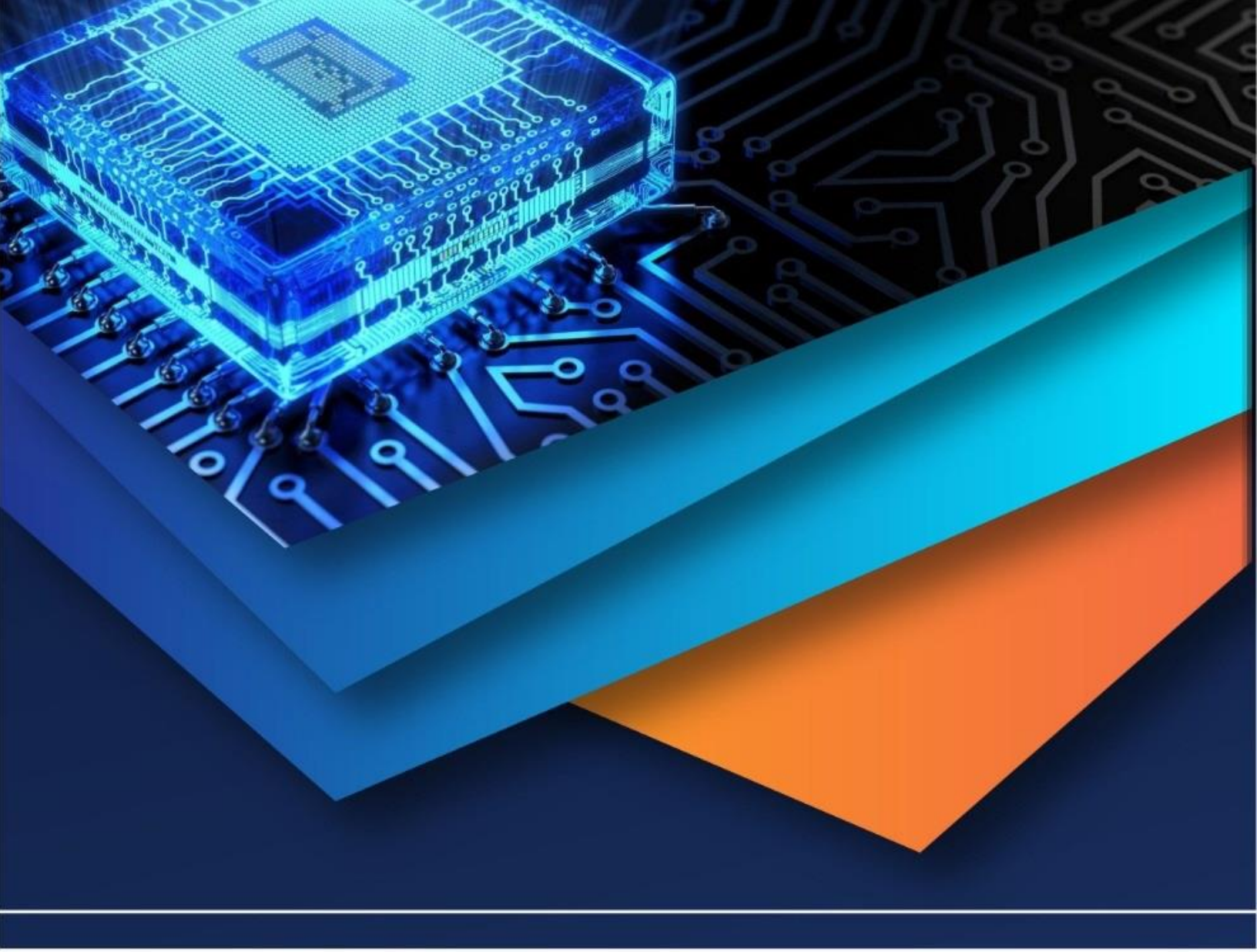

10.22214/IJRASET

45.98

IMPACT FACTOR: 7.129

IMPACT FACTOR: 7.429

INTERNATIONAL JOURNAL FOR RESEARCH

IN APPLIED SCIENCE & ENGINEERING TECHNOLOGY